

Supporting Information

[Ag₁₅H₁₃(DPPH)₅]²⁺ and [Ag₂₇H₂₂(DPPB)₇]³⁺: Two New Hydride and Phosphine Co-Protected Clusters and Their Fragmentation Leading to Naked Clusters, Ag₁₃⁺ and Ag₂₅⁺

Madhuri Jash, Esma Khatun, Papri Chakraborty, Chennu Sudhakar and Thalappil Pradeep*

DST Unit of Nanoscience (DST UNS) and Thematic Unit of Excellence (TUE), Department of Chemistry, Indian Institute of Technology Madras, Chennai 600 036, India

*To whom correspondence should be addressed. E-mail: pradeep@iitm.ac.in

Table of Contents

Name	Description	Page No.
S1	Characterization of [Ag ₁₅ D ₁₃ (DPPH) ₅] ²⁺ cluster	S3
S2	Time dependent UV-vis spectra of sample I during synthesis	S4
S3	Time dependent ESI MS of sample I during synthesis	S5
S4	¹ H NMR spectra of DPPH and [Ag ₁₅ H ₁₃ (DPPH) ₅] ²⁺ cluster	S6
S5	³¹ P NMR spectra of DPPH and [Ag ₁₅ H ₁₃ (DPPH) ₅] ²⁺ cluster	S7
S6	XPS spectra of [Ag ₁₅ H ₁₃ (DPPH) ₅] ²⁺ cluster	S8
S7	SEM EDS of [Ag ₁₅ H ₁₃ (DPPH) ₅] ²⁺ cluster	S9
S8	TEM analysis of [Ag ₁₅ H ₁₃ (DPPH) ₅] ²⁺ cluster	S10
S9	Comparison of the fragmentation pathway of [Ag ₁₅ H ₁₃ (DPPH) ₅] ²⁺ and [Ag ₁₅ D ₁₃ (DPPH) ₅] ²⁺ clusters	S11
S10	MS/MS of [Ag ₁₅ D ₁₃ (DPPH) ₅] ²⁺ cluster	S12
S11	Fragmentation pathway of [Ag ₁₅ H ₁₃ (DPPH) ₅] ²⁺ cluster	S13
S12	Characterization of [Ag ₂₇ D ₂₂ (DPPB) ₇] ³⁺ cluster	S14
S13	¹ H NMR spectra of DPPB and [Ag ₂₇ H ₂₂ (DPPB) ₇] ³⁺ cluster	S15
S14	³¹ P NMR spectra of DPPB and [Ag ₂₇ H ₂₂ (DPPB) ₇] ³⁺ cluster	S16
S15	XPS spectra of [Ag ₂₇ H ₂₂ (DPPB) ₇] ³⁺ cluster	S17
S16	SEM EDS of [Ag ₂₇ H ₂₂ (DPPB) ₇] ³⁺ cluster	S18
S17	TEM analysis of [Ag ₂₇ H ₂₂ (DPPB) ₇] ³⁺ cluster	S19

S18	Comparison between the experimental and calculated spectra of Ag_{25}^+	S20
S19	Fragmentation pathway of $[\text{Ag}_{27}\text{H}_{22}(\text{DPPB})_7]^{3+}$ cluster	S21

Supporting information 1

Characterization of $[\text{Ag}_{15}\text{D}_{13}(\text{DPPH})_5]^{2+}$ cluster:

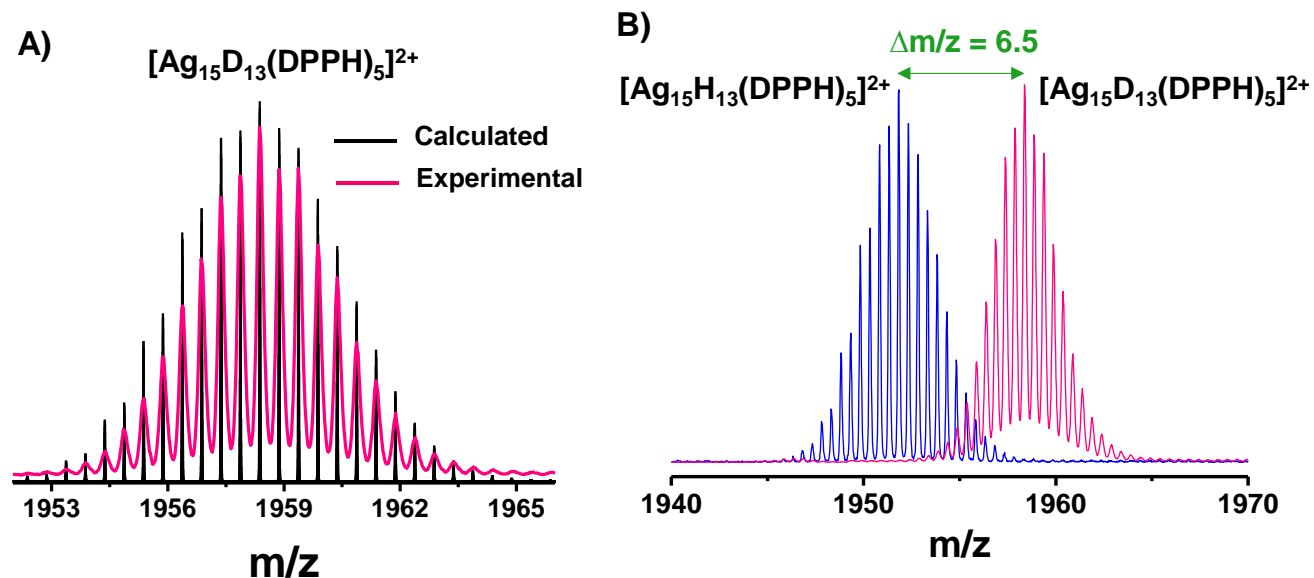


Figure S1. (A) Experimental mass spectrum (pink trace) of $[\text{Ag}_{15}\text{D}_{13}(\text{DPPH})_5]^{2+}$ cluster match well with its calculated (black trace) isotopic pattern. (B) The ESI MS of $[\text{Ag}_{15}\text{H}_{13}(\text{DPPH})_5]^{2+}$ and $[\text{Ag}_{15}\text{D}_{13}(\text{DPPH})_5]^{2+}$ showing the mass shift due to the exchange of hydrogen atoms with deuterium atoms.

Supporting information 2

Time dependent UV-vis spectra of sample I during synthesis:

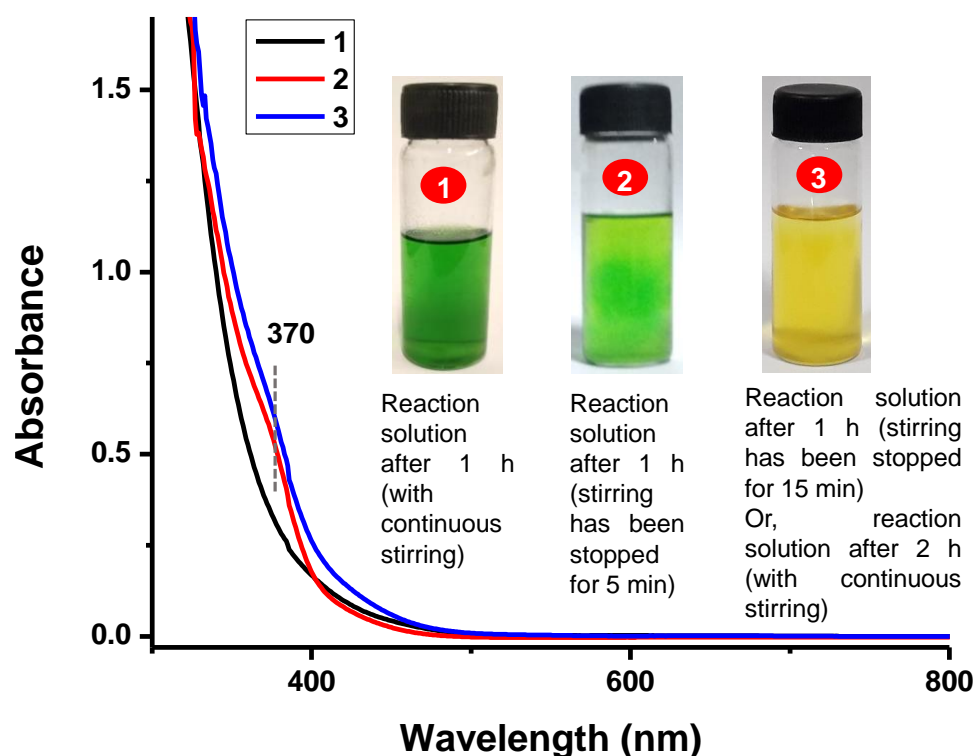


Figure S2. Time dependent UV-vis spectra during the synthesis of sample I with their corresponding photographs in inset. The photographs show that during 1 h of synthesis with continuous stirring, the color of the solution remains green (1). Whereas, by stopping the stirring after 1 h, the color changed immediately from green to yellowish green within 5 min (2). After 15 min of stopping stirring, the color became fully dark yellow (3). The bottle labeled 3 also represents the same solution when the reaction was continuously stirred for 2 h.

Supporting information 3

Time dependent ESI MS of sample I during synthesis:

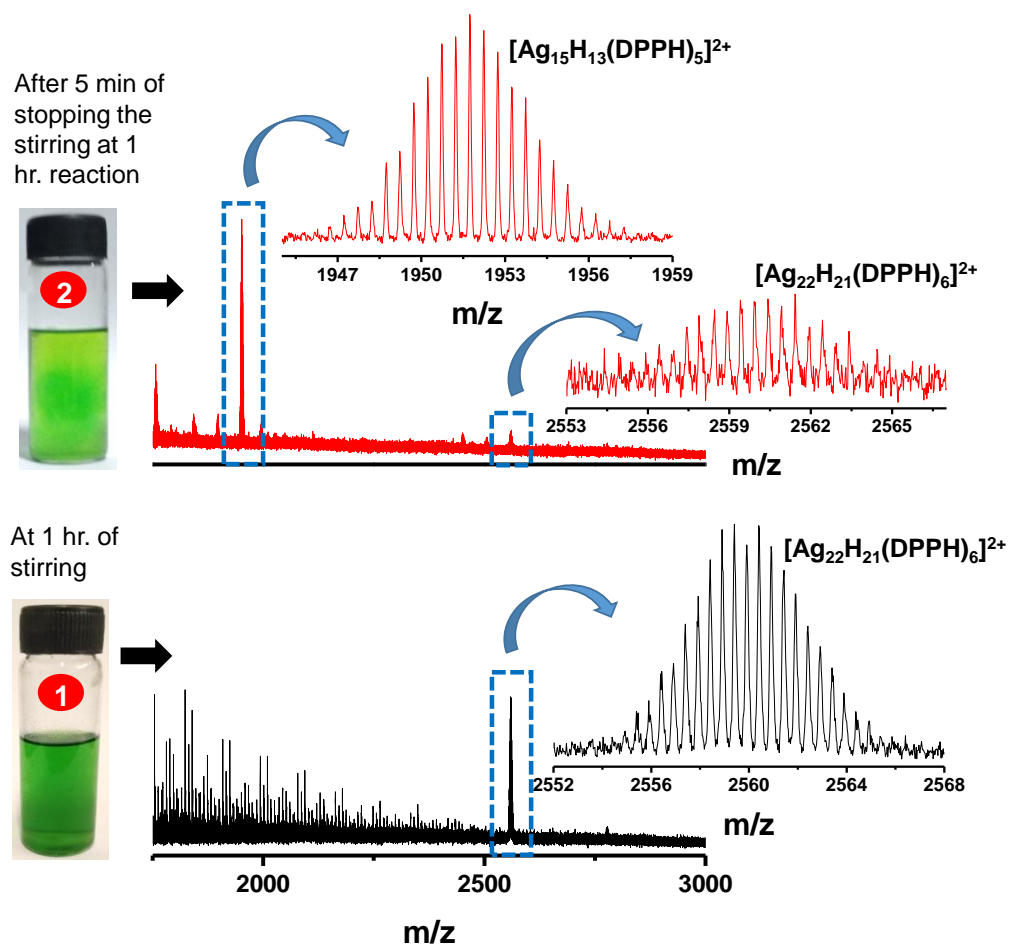


Figure S3. Time dependent ESI MS during the synthesis of sample **I** with their corresponding photographs (on the left). The ESI MS of green solution (1) shows the presence of $[Ag_{22}H_{21}(DPPH)_6]^{2+}$ cluster during 1 h stirring. Whereas, after 5 min of stopping the stirring the green color was converted to yellowish green (2) and the intensity of $[Ag_{22}H_{21}(DPPH)_6]^{2+}$ decreased significantly in the ESI MS along with increased intensity of $[Ag_{15}H_{13}(DPPH)_5]^{2+}$ (sample **I**).

Supporting information 4

^1H NMR spectra of DPPH and $[\text{Ag}_{15}\text{H}_{13}(\text{DPPH})_5]^{2+}$ cluster:

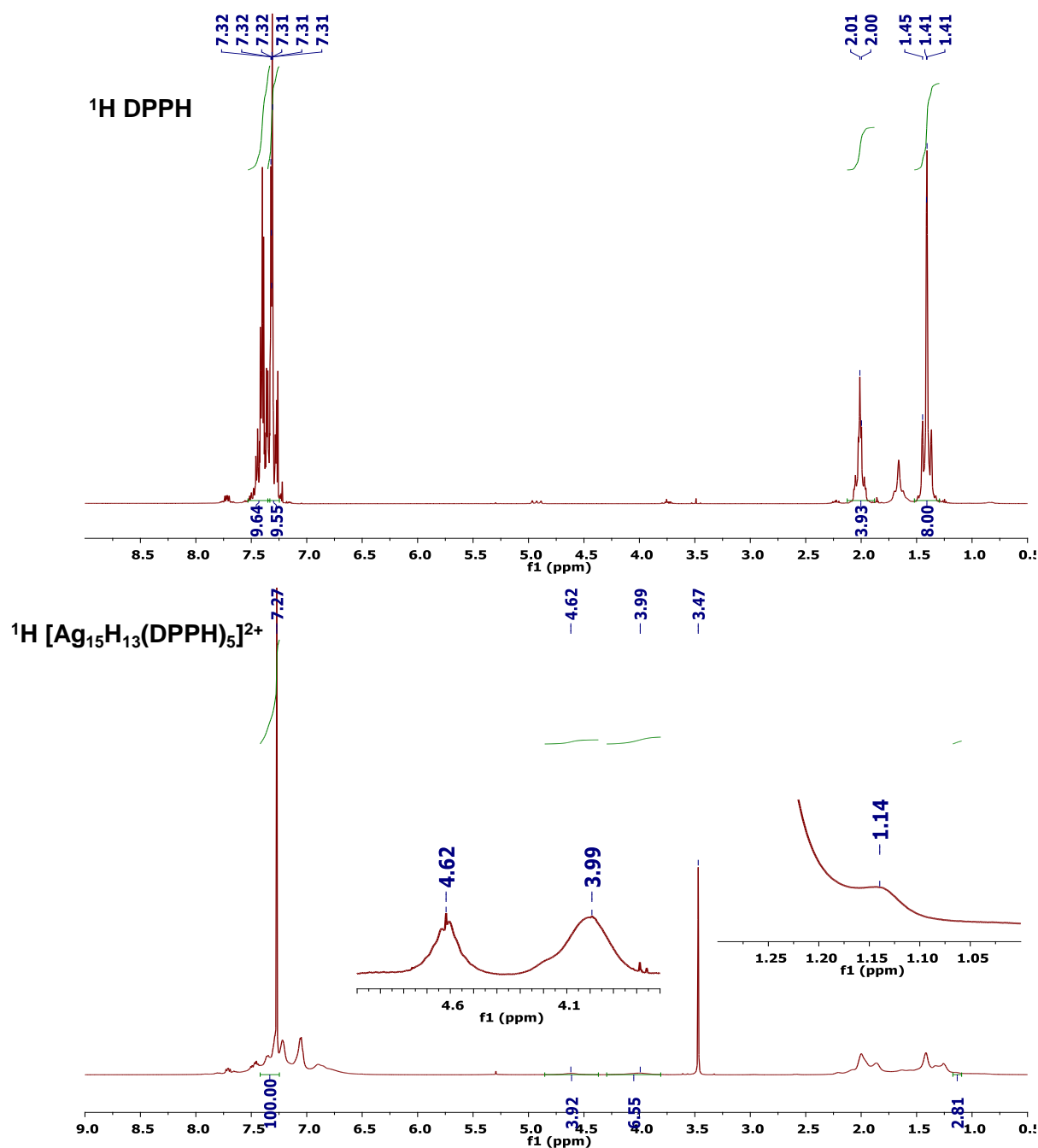


Figure S4. ^1H NMR spectra of DPPH and $[\text{Ag}_{15}\text{H}_{13}(\text{DPPH})_5]^{2+}$ clusters. Broad peaks of $[\text{Ag}_{15}\text{H}_{13}(\text{DPPH})_5]^{2+}$ at 1.14, 3.99 and 4.62 ppm confirm the presence of hydride protected clusters.

Supporting information 5

^{31}P NMR spectra of DPPH and $[\text{Ag}_{15}\text{H}_{13}(\text{DPPH})_5]^{2+}$ cluster:

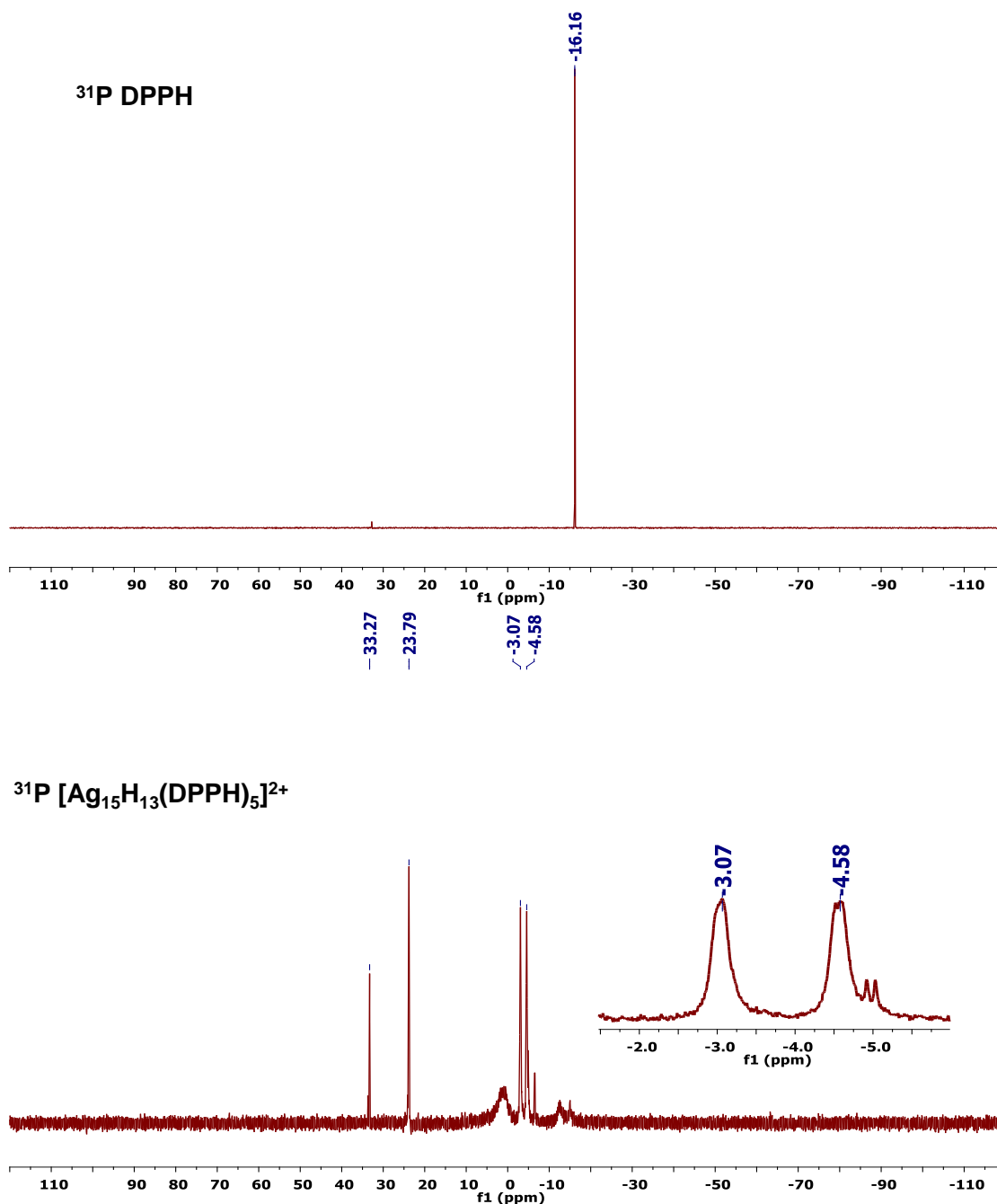


Figure S5. ^{31}P NMR spectra of DPPH and $[\text{Ag}_{15}\text{H}_{13}(\text{DPPH})_5]^{2+}$ clusters. The ^{31}P signal at -16.16 ppm for DPPH ligand disappears in the $[\text{Ag}_{15}\text{H}_{13}(\text{DPPH})_5]^{2+}$ cluster due to the binding of ligands with metal core, which is also confirmed by the appearance of new broad peaks at -4.58 and -3.07 ppm in the nanoclusters. Peaks at 23.79 and 33.27 ppm are due to phosphine oxides.

Supporting information 6

XPS spectra of $[\text{Ag}_{15}\text{H}_{13}(\text{DPPH})_5]^{2+}$ cluster:

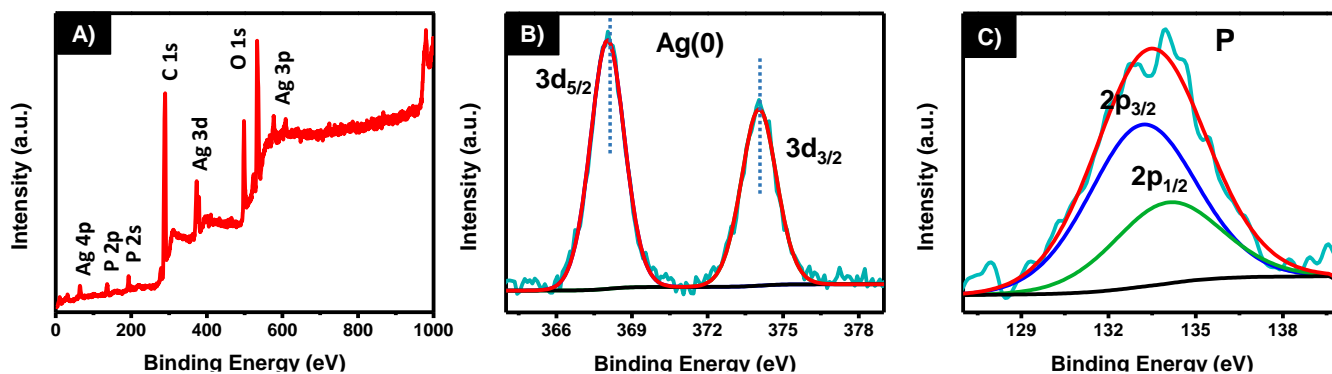


Figure S6. (A) XPS survey spectrum of $[\text{Ag}_{15}\text{H}_{13}(\text{DPPH})_5]^{2+}$ showing all the expected elements (Ag, P and C). (B) The Ag 3d region. Ag 3d_{5/2} at 368.04 eV indicates the presence of Ag(0) state. (C) P 2p region of the nanocluster. P 2p_{3/2} appears at 133.24 eV.

Supporting information 7

SEM EDS of $[\text{Ag}_{15}\text{H}_{13}(\text{DPPH})_5]^{2+}$ cluster:

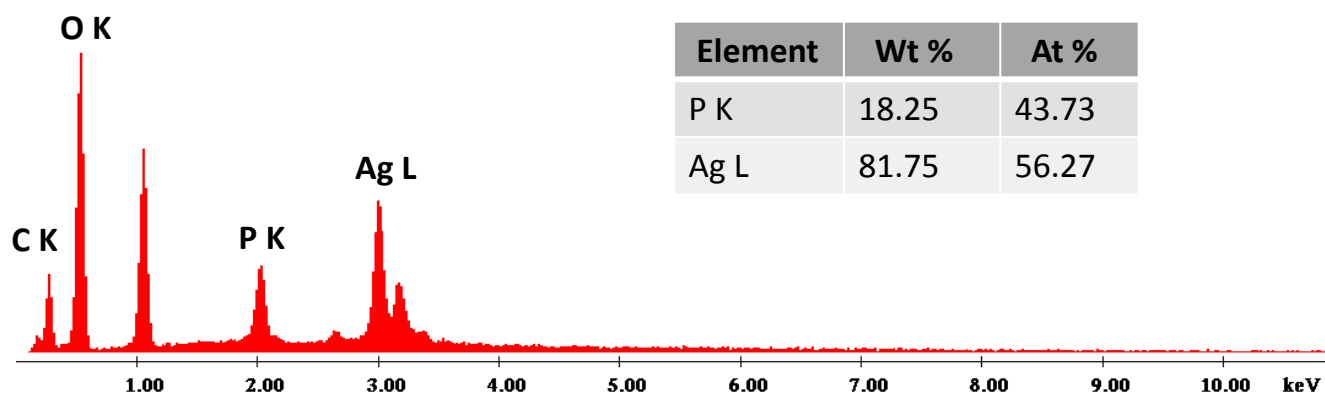


Figure S7. SEM EDS of $[\text{Ag}_{15}\text{H}_{13}(\text{DPPH})_5]^{2+}$ cluster with quantification of elements. Ag:P atomic ratio matches well with the Ag:P ratio obtained from the molecular formula of the cluster.

Supporting information 8

TEM analysis of $[\text{Ag}_{15}\text{H}_{13}(\text{DPPH})_5]^{2+}$ cluster:

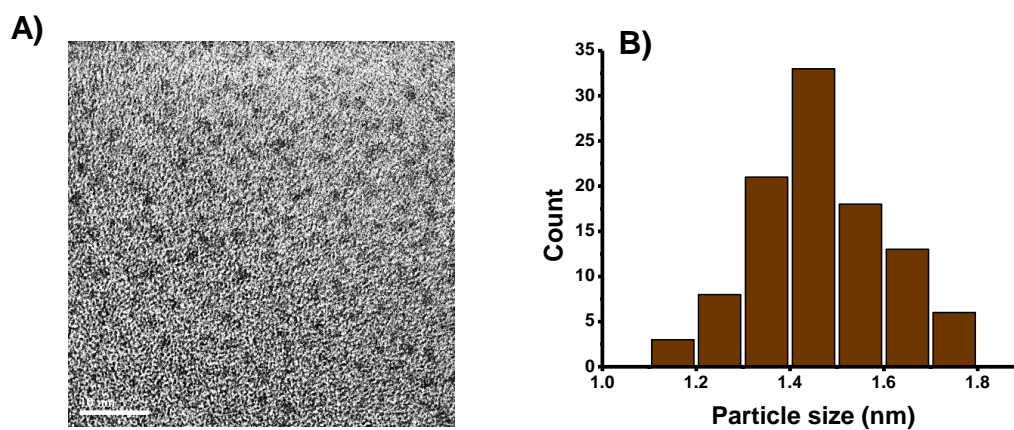


Figure S8. (A) TEM image of the $[\text{Ag}_{15}\text{H}_{13}(\text{DPPH})_5]^{2+}$ cluster. Scale bar is 10 nm. (B) Particle distribution shows an average size of 1.46 ± 0.13 nm for this nanocluster.

Supporting information 9

Comparison of the fragmentation pathway of $[\text{Ag}_{15}\text{H}_{13}(\text{DPPH})_5]^{2+}$ and $[\text{Ag}_{15}\text{D}_{13}(\text{DPPH})_5]^{2+}$ clusters:

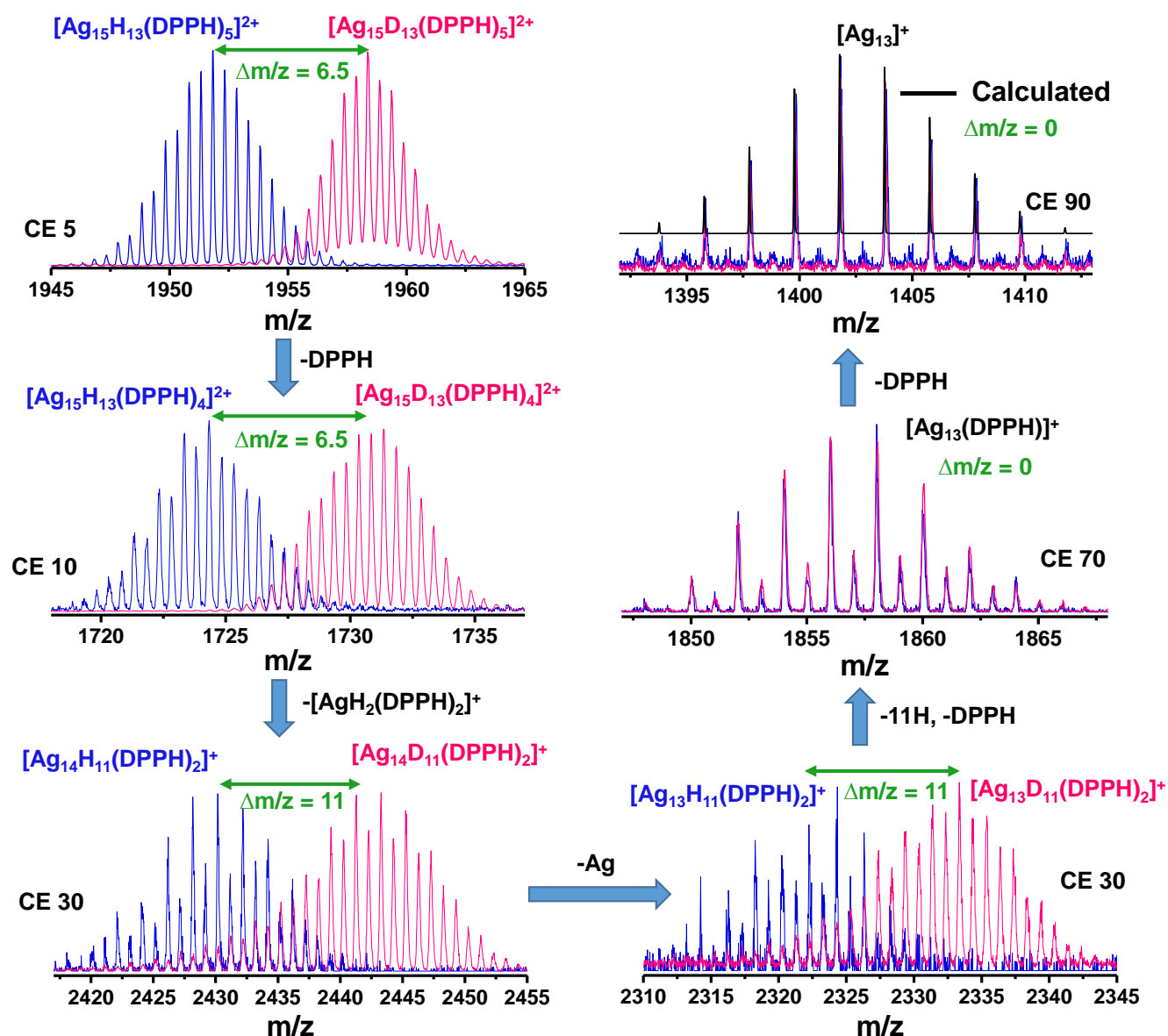


Figure S9. Expanded ESI MS of $[\text{Ag}_{15}\text{H}_{13}(\text{DPPH})_5]^{2+}$ (blue trace) and $[\text{Ag}_{15}\text{D}_{13}(\text{DPPH})_5]^{2+}$ (pink trace) at different collision energies during the formation of naked cluster, Ag_{13}^{+} by another possible pathway. The mass shift ($\Delta m/z$) in between the blue and pink traces confirms the presence of hydrogen in the particular fragmented ions. The isotopic distribution of Ag_{13}^{+} confirms the absence of hydrogen atoms, which also matches with the calculated pattern (black trace).

Supporting information 10

MS/MS of $[\text{Ag}_{15}\text{D}_{13}(\text{DPPH})_5]^{2+}$ cluster:

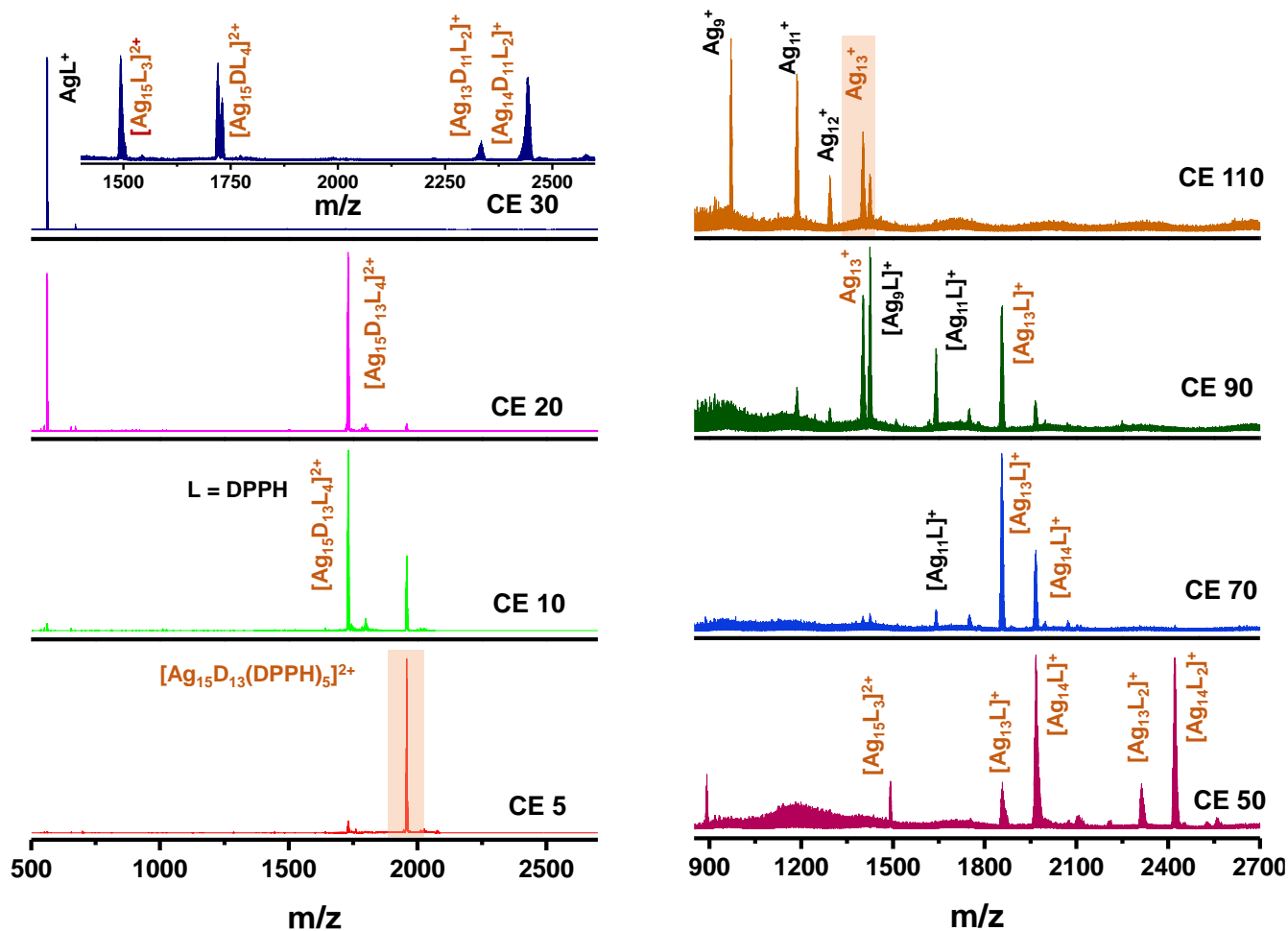


Figure S10. Collision energy dependent MS/MS spectra of the $[\text{Ag}_{15}\text{D}_{13}(\text{DPPH})_5]^{2+}$ cluster. Increase in collision energy from 5 to 110 (in instrumental units) results in the detachment of deuterium, DPPH and $[\text{AgDPPH}]^+$ from $[\text{Ag}_{15}\text{D}_{13}(\text{DPPH})_5]^{2+}$ resulting in Ag_{13}^+ . Fragments labeled in brown lead to the formation of naked cluster, Ag_{13}^+ .

Supporting information 11

Fragmentation pathway of $[\text{Ag}_{15}\text{H}_{13}(\text{DPPH})_5]^{2+}$ cluster:

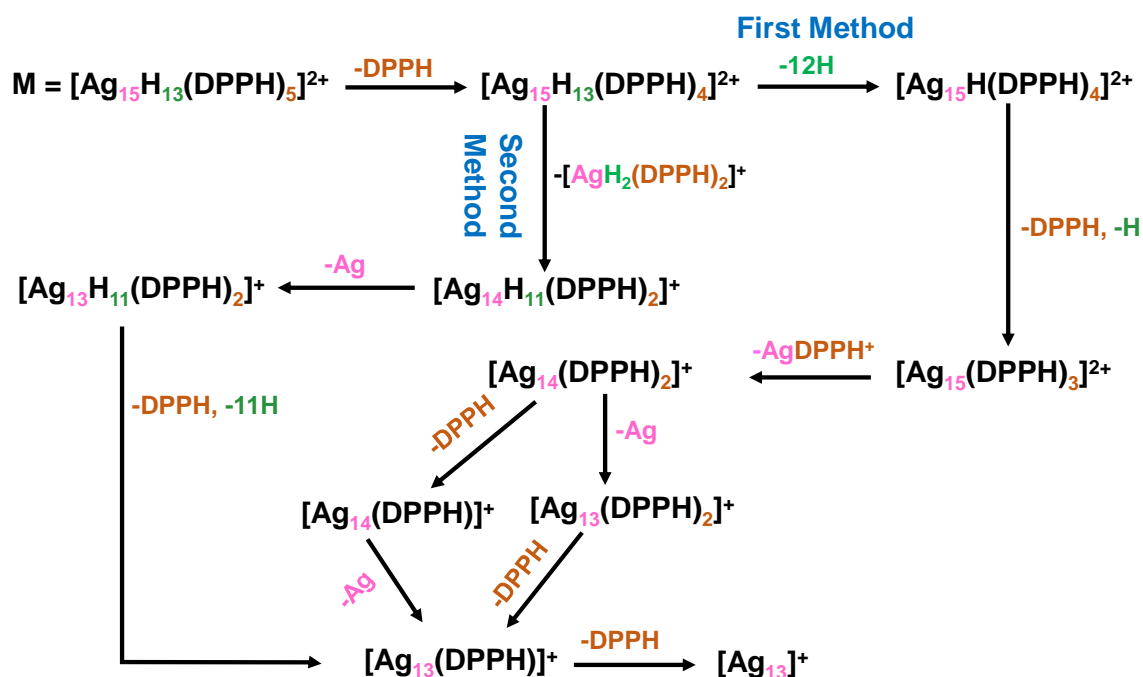


Figure S11. Collision energy dependent fragmentation pathway of $[\text{Ag}_{15}\text{H}_{13}(\text{DPPH})_5]^{2+}$ cluster towards the formation of naked cluster, Ag_{13}^+ . Hydrogen and DPPH loss do not involve any alternation of charge state of the resulting cluster. Whereas, $[\text{AgDPPH}]^+$ loss results in the reduction of charge state from +2 to +1.

Supporting information 12

Characterization of $[\text{Ag}_{27}\text{D}_{22}(\text{DPPB})_7]^{3+}$ cluster:

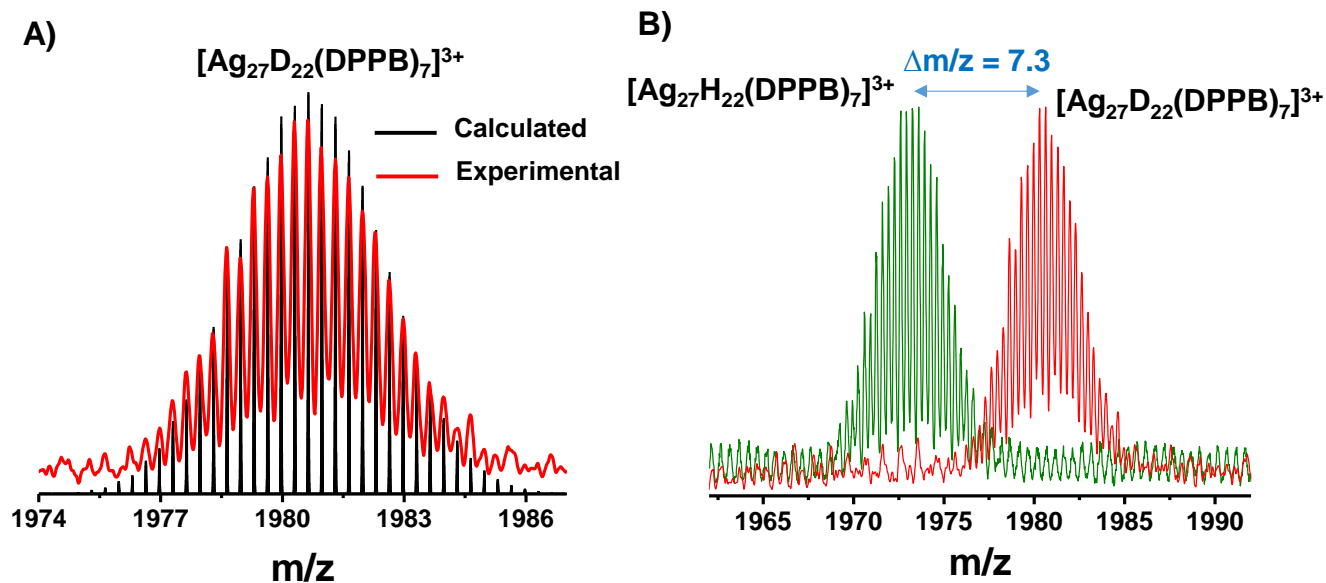


Figure S12. (A) Experimental mass spectrum (red trace) of $[\text{Ag}_{27}\text{D}_{22}(\text{DPPB})_7]^{3+}$ cluster and it matches well with its calculated (black trace) isotopic pattern. (B) The ESI MS of $[\text{Ag}_{27}\text{H}_{22}(\text{DPPB})_7]^{3+}$ and $[\text{Ag}_{27}\text{D}_{22}(\text{DPPB})_7]^{3+}$ showing a mass shift due to the exchange of hydrogen atoms with deuterium atoms.

Supporting information 13

^1H NMR spectra of DPPB and $[\text{Ag}_{27}\text{H}_{22}(\text{DPPB})_7]^{3+}$ cluster:

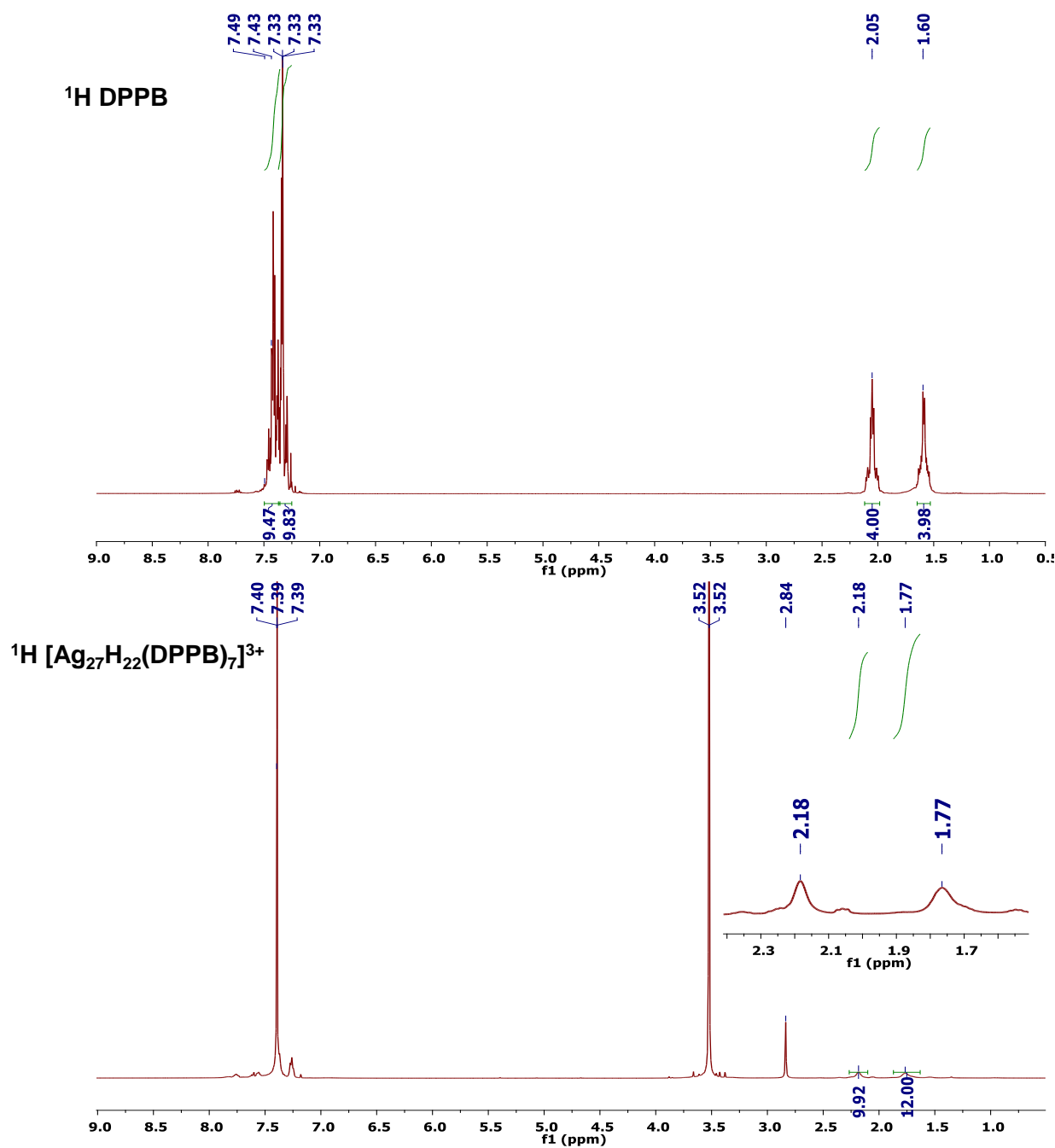


Figure S13. ^1H NMR spectra of DPPB and $[\text{Ag}_{27}\text{H}_{22}(\text{DPPB})_7]^{3+}$ clusters. Broad peaks of $[\text{Ag}_{27}\text{H}_{22}(\text{DPPB})_7]^{3+}$ at 1.77 and 2.18 ppm confirm the presence of hydride protected nanoclusters.

Supporting information 14

^{31}P NMR spectra of DPPB and $[\text{Ag}_{27}\text{H}_{22}(\text{DPPB})_7]^{3+}$ cluster:

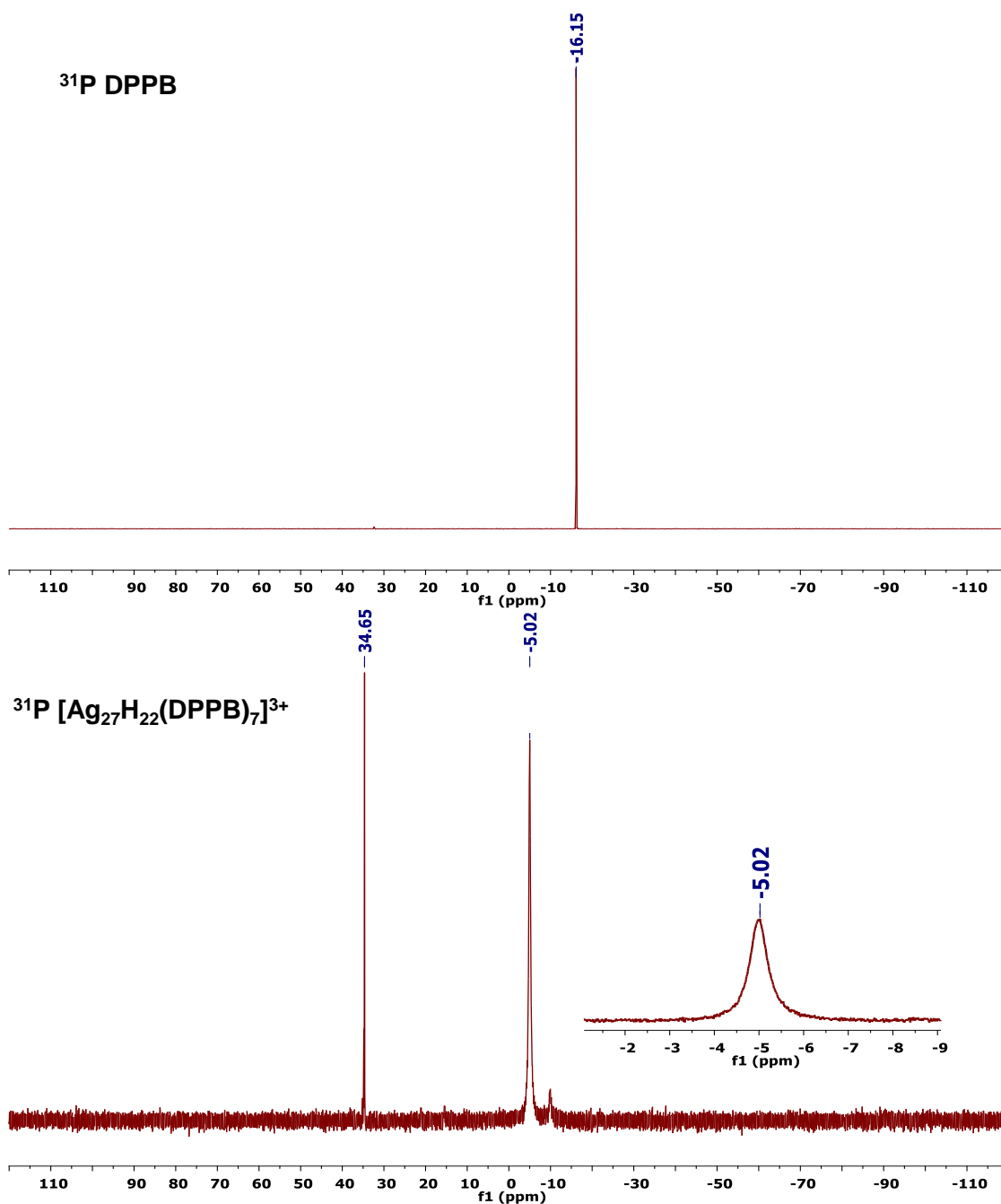


Figure S14. ^{31}P NMR spectra of DPPB and $[\text{Ag}_{27}\text{H}_{22}(\text{DPPB})_7]^{3+}$ clusters. The ^{31}P signal at -16.15 ppm for DPPB ligand disappears in the $[\text{Ag}_{27}\text{H}_{22}(\text{DPPB})_7]^{3+}$ cluster due to the binding of ligands with the metal core, which is also confirmed by the appearance of new broad peaks at -5.02 ppm in the nanoclusters. Peak at 34.65 ppm is due to phosphine oxides.

Supporting information 15

XPS spectra of $[\text{Ag}_{27}\text{H}_{22}(\text{DPPB})_7]^{3+}$ cluster:

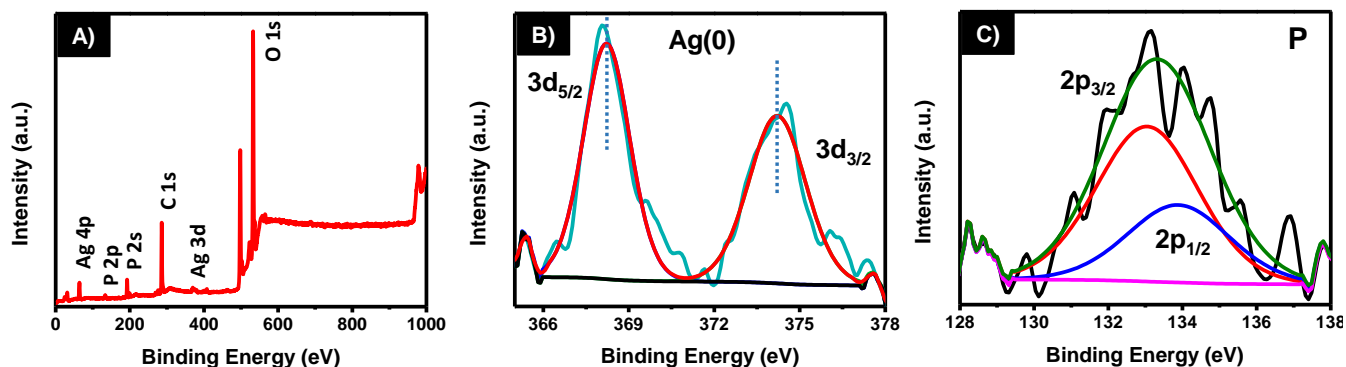


Figure S15. (A) XPS survey spectrum of $[\text{Ag}_{27}\text{H}_{22}(\text{DPPB})_7]^{3+}$ showing all the expected elements (Ag, P and C). (B) Ag 3d spectrum of the nanocluster. Ag $3d_{5/2}$ appears at 368.22 eV indicating the presence of Ag(0) state. (C) P 2p spectrum of the nanocluster. P $2p_{3/2}$ appears at 133.03 eV.

Supporting information 16

SEM EDS of $[\text{Ag}_{27}\text{H}_{22}(\text{DPPB})_7]^{3+}$ cluster:

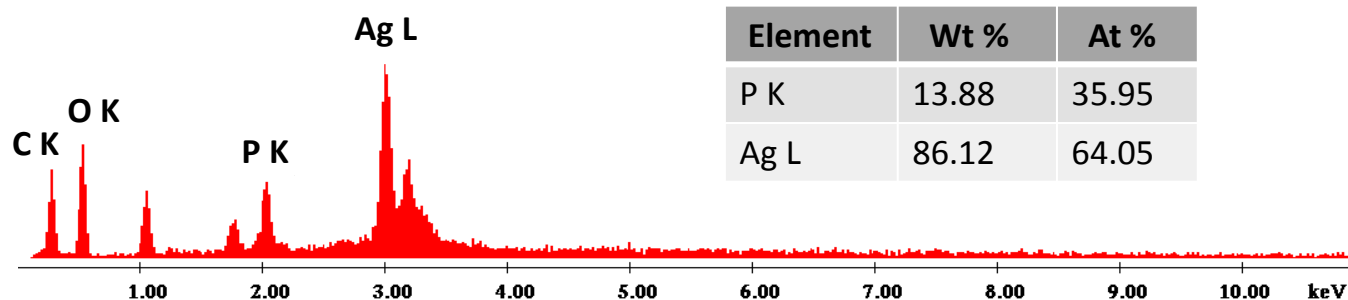


Figure S16. SEM EDS of $[\text{Ag}_{27}\text{H}_{22}(\text{DPPB})_7]^{3+}$ cluster with quantification of elements. Ag:P atomic ratio matches well with the Ag:P ratio obtained from the molecular formula of the cluster.

Supporting information 17

TEM analysis of $[\text{Ag}_{27}\text{H}_{22}(\text{DPPB})_7]^{3+}$ cluster:

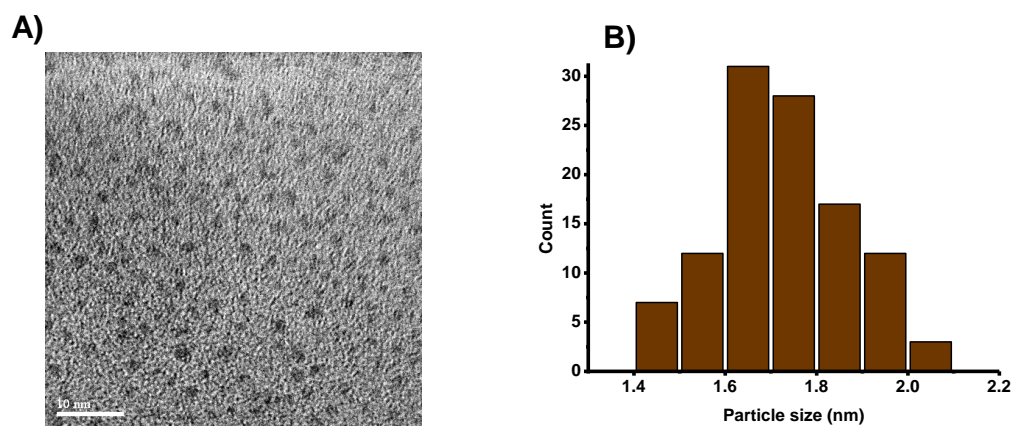


Figure S17. (A) TEM image of the $[\text{Ag}_{27}\text{H}_{22}(\text{DPPB})_7]^{3+}$ cluster. Scale bar is 10 nm. (B) Particle distribution shows an average size of 1.72 ± 0.14 nm for this nanocluster.

Supporting information 18

Comparison between the experimental and the calculated spectra of Ag_{25}^+ :

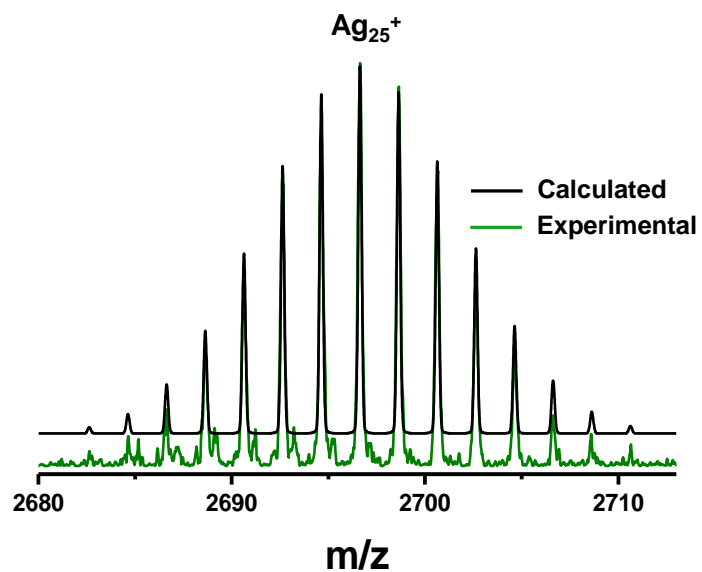


Figure S18. Experimental mass spectrum (green trace) of Ag_{25}^+ matches well with the calculated (black trace) isotopic pattern.

Supporting information 19

Fragmentation pathway of $[\text{Ag}_{27}\text{H}_{22}(\text{DPPB})_7]^{3+}$ cluster:

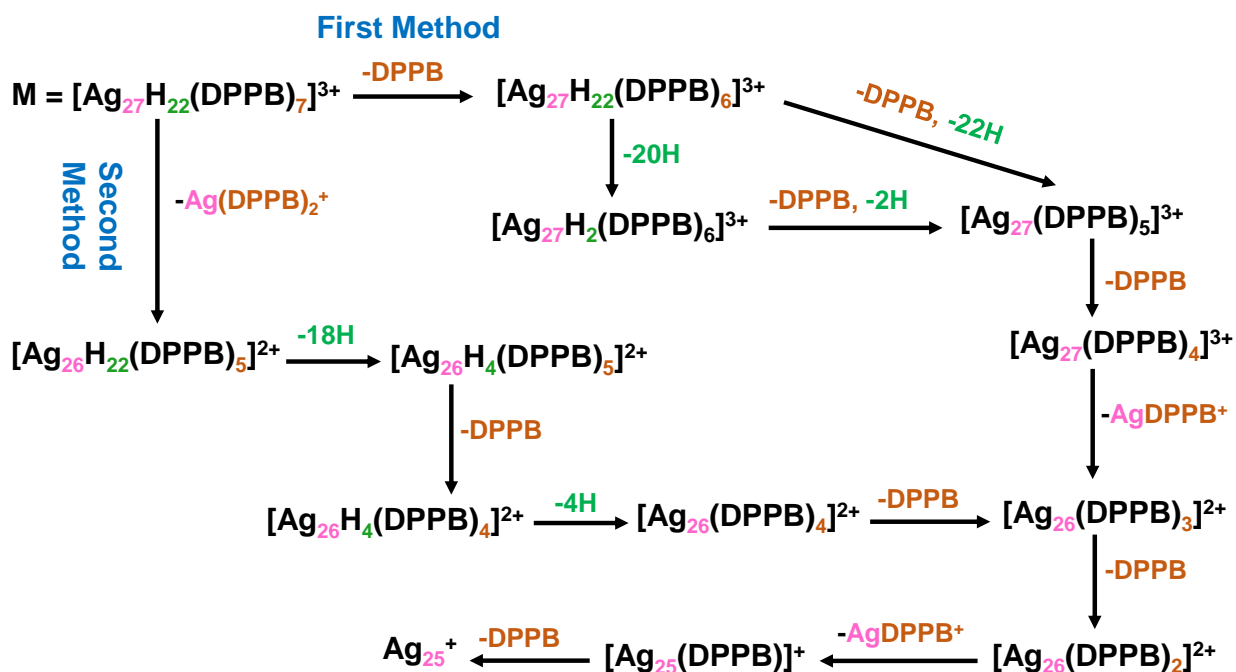


Figure S19. Collision energy dependent fragmentation pathway of $[\text{Ag}_{27}\text{H}_{22}(\text{DPPB})_7]^{3+}$ cluster towards the formation of naked cluster, Ag_{25}^+ . Hydrogen and DPPB loss do not involve any alternation of charge state of the resulting cluster. Whereas, $[\text{AgDPPB}]^+$ loss results in the reduction of charge state from +3 to +2 and from +2 to +1.